

# Fermion induced superfluid decoherence in the boson Hubbard model on an optical lattice

Roman M. Lutchyn<sup>1</sup>, Sumanta Tewari<sup>2</sup>, and S. Das Sarma<sup>1</sup>

<sup>1</sup>*Condensed Matter Theory Center and Joint Quantum Institute,*

*Department of Physics, University of Maryland, College Park, MD 20742 and*

<sup>2</sup>*Department of Physics and Astronomy, Clemson University, Clemson, SC 29634*

(Dated: December 12, 2018)

We study the phase diagram of a degenerate gas of bosons in an optical lattice, described by the boson Hubbard Hamiltonian, interacting with spin-polarized fermions. Virtual transitions of the bosons to the higher Bloch bands, coupled with the contact interspecies interactions of either sign, result in an effective increase of the bosonic on-site repulsion. If this renormalization of the on-site potential is dominant over the fermionic screening of the boson interactions, superfluid coherence of the Bose-Hubbard system will be reduced by the fermions. We discuss experimental implications for cold atomic systems.

PACS numbers: 03.75.-b, 03.75.Gg, 03.75.Mn, 03.75.Lm

*Introduction:* The intrinsic effect of introducing a gas of fermions (excluding heating effect) on the famous superfluid-insulator (SI) phase diagram [1] of the boson Hubbard model is still theoretically unresolved. Experimentally, the situation is quite unambiguous: the addition of a degenerate gas of spin-polarized fermions to the bosonic superfluid condensate reduces the superfluid coherence, *irrespective of the sign* of the interaction between the bosons and the fermions. This indicates that the condensate, in the presence of interactions with the fermions, gives way to the Mott insulating phase at values of the effective  $t/U$  larger than that without the fermions, where  $t$  is the nearest neighbor hopping amplitude and  $U$  is the on-site interaction of the constituent bosons. The areas of the Mott insulating lobes in the boson Hubbard phase diagram are thus enhanced by the fermions. The earlier experiments [2, 3] observed the loss of superfluid coherence for fixed attractive boson-fermion interactions,  $U_{BF}$ , which were larger in magnitude than the boson on-site repulsion itself. Recently this finding has also been confirmed for both attractive and repulsive interspecies interactions in a range of values for  $|U_{BF}|$  both smaller and larger than  $U$  [4]. While the problem of the Bose-Fermi mixture is theoretically interesting for the ensuing complexity in the phase diagram [5, 6, 7, 8, 9, 10, 11, 12, 13, 14], the main experimental observation – a suppression of the superfluid coherence by adding fermions – is contrary to many recent theoretical studies [5, 12, 14]; the only notable exception is the numerical work in Ref. [15].

In the theoretical studies of the SI phase diagram of the Bose-Fermi mixture [5, 12, 13, 14], the central argument involves the screening of the boson on-site repulsive potential by the fermions. The mobile fermions mediate a spatially and temporally non-local *attractive* interaction among the bosons, which can be shown to screen and reduce the repulsive interaction  $U$  of the boson Hubbard model. Since the on-site repulsion tends to localize the

bosons on the individual lattice sites (favoring the Mott insulating phases for any integer filling factor), any reduction of this interaction, such as that provided by the fermionic screening, should expand the area occupied by the superfluid phase in the phase diagram [5, 12, 14]. As pointed out before, this simple intuitive picture, made rigorous recently both numerically [12] and analytically [14] on the single band boson Hubbard model, cannot explain the available experiments. Here we show that there is an additional effect of the fermion contact interactions of either sign, mediated by virtual transitions of the bosons to the higher Bloch bands, which leads to an effective *increase* of the boson on-site interactions. There is some numerical evidence of this effect [15] for the case of attractive interspecies interactions only. In this Letter, we treat the above two disparate effects within a unified analytical framework. We believe that this theory, which includes the idea of virtual transitions to the higher boson Bloch bands, provides an explanation for the loss of bosonic superfluid coherence by introducing fermions (irrespective of the sign of the interspecies interactions), seen in the recent cold atom experiments.

To get a unified description of the effects of the fermions, we start with the multi-band boson Hubbard model where the two lowest-lying boson Bloch bands are separated by an energy gap  $\Omega \gg t, \mu, U$ , where  $\mu$  is the boson chemical potential. We assume that the fermions are coupled to the bosons in the two lowest-lying Bloch bands with contact interactions. The trivial effects of the presence of the higher boson bands are renormalizations of the bare bosonic parameters  $t, \mu, U$ , which are present even without the fermions (and hence, will be mostly suppressed here). However, most importantly, we find that the virtual transitions of the bosons to the higher Bloch bands give rise to a new type of on-site *repulsive* interaction among the bosons mediated by the fermions. This interaction, which is linear in  $U_{BF}$  to the leading order, but, surprisingly, remains repulsive for either sign

of  $U_{BF}$ , tends to hinder the flow of the bosons on the optical lattice. Thus, this interaction moves the Mott insulating transitions to shallower lattice depths for any boson integer filling factor. Including this new interaction and the usual fermion-mediated screening interaction [5, 12, 13, 14] in a unified framework [14], we find that the question of the overall shift of the phase diagram is a quantitative one arising from a competition between attractive and repulsive terms: if the fermion-induced higher-band renormalization of the on-site potential is dominant, as may be the case in the recent experiments, superfluid coherence will be reduced by introducing the fermions.

*Model:* We begin with the following second quantized Hamiltonian describing the bosons and a gas of spin-polarized fermions interacting with each other through a contact interaction in an optical lattice:

$$H = \int d^3\mathbf{r} \Phi^\dagger(\mathbf{r}) \left[ H_0^B + \frac{g_{BB}}{2} \Phi^\dagger(\mathbf{r}) \Phi(\mathbf{r}) \right] \Phi(\mathbf{r}) + \int d^3\mathbf{r} \Psi^\dagger(\mathbf{r}) H_0^F \Psi(\mathbf{r}) + \frac{g_{BF}}{2} \int d^d\mathbf{r} \Phi^\dagger(\mathbf{r}) \Phi(\mathbf{r}) \Psi^\dagger(\mathbf{r}) \Psi(\mathbf{r}). \quad (1)$$

Here,  $\Phi(\mathbf{r})$  and  $\Psi(\mathbf{r})$  are the field operators for the bosonic and the fermionic atoms, respectively, the single particle Hamiltonians  $H_0^{B/F} = \hat{T}_{B/F} + V_{\text{lat}}(\mathbf{r})$ , with  $\hat{T}_{B/F}$  representing the kinetic energy for the bosons/fermions and  $V_{\text{lat}}(\mathbf{r})$  denoting the lattice potential,  $V_{\text{lat}}(\mathbf{r}) = \sum_{j=1}^3 V_0 \sin^2(\pi \frac{r_j}{a})$  with  $a$  as the lattice spacing. The interaction coupling constants are given by  $g_{BB} = \frac{4\pi a_{BB}}{m_B}$ ,  $g_{BF} = \frac{4\pi a_{BF}}{m_{\text{red}}}$ , where  $m_B$  is the mass of a bosonic atom,  $m_{\text{red}}$  is the boson-fermion reduced mass and  $a_{BB/BF}$  are the boson-boson and boson-fermion scattering lengths, respectively.

We now expand the field operators in the Wannier function basis,  $\Phi(\mathbf{r}) = \sum_{i,\alpha} b_{i,\alpha} w_\alpha(\mathbf{r} - \mathbf{r}_i)$ , and  $\Psi(\mathbf{r}) = \sum_{i,\alpha} u_\alpha(\mathbf{r} - \mathbf{r}_i) c_{i,\alpha}$ , where the operators  $b_{i,\alpha}$  and  $c_{i,\alpha}$  annihilate the bosons and the fermions at a site  $i$  in a band  $\alpha$ , respectively. Substituting the above expressions for the field operators into Eq. (1), one obtains the full multi-band model [16, 17, 18] for the Bose-Fermi system. Instead of treating the complexity of the full multi-band Hamiltonian, we consider, for simplicity, a two-band model for the bosons with the fermions being in a single band, and keep the largest band-mixing terms in the bosonic part of the Hamiltonian. This effective two-band model for the bosons, which can be justified for large interband energy separation  $\Omega = \sqrt{4E_R V_0}$ , where  $E_R = \pi^2/2m_B a^2$  is the recoil energy, captures the essential physics involving the virtual transitions of the bosons to the higher Bloch bands. The fermion Wannier wavefunctions  $u_\alpha(\mathbf{r} - \mathbf{r}_i)$  are chosen using the mean-field one-body Hamiltonian for the fermions,  $\hat{T}_F + V_F(\mathbf{r})$ , where the effective potential  $V_F(\mathbf{r}) = V_{\text{lat}}(\mathbf{r}) + \frac{g_{BF}}{2} \rho_B(\mathbf{r})$ . Here,  $\rho_B(\mathbf{r})$  is the average boson density per site. Thus, the shapes of these functions within a unit cell, which will

be important later to determine the sign of the fermion renormalization of the on-site bosonic potential (see the discussion after Eq. (6)), depend on the sign of the inter-species interactions (sign of  $a_{BF}$ ). In the rest of the paper we will study the two-band Bose-Fermi model defined by the Hamiltonian,

$$\begin{aligned} H &= H_l + H'_l + H_t + H_{BF} + H_F \quad (2) \\ H_l &= \sum_{i,\alpha} \left[ \varepsilon_\alpha \hat{n}_{i,\alpha} + \frac{U^{\alpha,\alpha}}{2} \hat{n}_{i,\alpha} (\hat{n}_{i,\alpha} - 1) \right] + \sum_{i,\alpha>\alpha'} 2U^{\alpha,\alpha'} \hat{n}_{i,\alpha} \hat{n}_{i,\alpha'} \\ H'_l &= \sum_{i,\alpha>\alpha'} \frac{U^{\alpha,\alpha'}}{2} \left[ b_{i,\alpha}^\dagger b_{i,\alpha'}^\dagger b_{i,\alpha} b_{i,\alpha'} + b_{i,\alpha}^\dagger b_{i,\alpha'}^\dagger b_{i,\alpha'} b_{i,\alpha} \right] \\ H_t &= - \sum_{\langle ij \rangle, \alpha} t^\alpha \left[ b_{i,\alpha}^\dagger b_{j,\alpha} + \text{H.c.} \right]; H_{BF} = \sum_{i,\alpha} U_{FB}^\alpha [\hat{n}_{i,\alpha} - \langle \hat{n}_{i,\alpha} \rangle] \hat{n}_i^F \\ H_F &= \sum_{\langle ij \rangle} \left[ \epsilon_0 \hat{n}_i^F \delta_{ij} - t_F (c_i^\dagger c_j + \text{H.c.}) \right], \end{aligned}$$

Here, the energies  $\varepsilon_\alpha = \langle w_{i,\alpha} | H_0^B | w_{i,\alpha} \rangle - \mu$ , the matrix elements  $U^{\alpha,\alpha'} = g_{BB} \langle w_{i,\alpha}; w_{i,\alpha'} | w_{i,\alpha}; w_{i,\alpha'} \rangle$  and  $U_{FB}^\alpha = g_{BF}/2 \langle w_{i,\alpha}; u_i | w_{i,\alpha}; u_i \rangle$ . The fermionic energy and hopping are given by  $\epsilon_0 = \langle u_i | \hat{T}_F + V_F(\mathbf{r}) | u_i \rangle - \mu$  and  $t_F = -\langle u_i | \hat{T}_F + V_F(\mathbf{r}) | u_j \rangle$ . We notice that the piece of the Hamiltonian  $H'_l$  in Eq. (2), which corresponds to scattering of the bosons between the first and the second Bloch bands, leads to band mixing. As we show below, these band-mixing terms, coupled with the fermion contact interactions in both bands, renormalize the local repulsive interaction between the constituent bosons in the low energy subspace.

*Schrieffer-Wolff transformation:* In order to reveal the nature of the renormalization, one needs to diagonalize the full Hamiltonian and project it on the subspace of the lower band only. Assuming that  $\Omega$  is the largest energy scale in the problem, we perform the Schrieffer-Wolff canonical transformation [19] on the Hamiltonian  $H$  to decouple the diagonal (boson number-conserving) and the non-diagonal (band-mixing) pieces of the Hamiltonian to a given order in  $1/\Omega$ :

$$H_{\text{eff}} = e^S H e^{-S} = H + [S, H] + \frac{1}{2} [S, [S, H]] + \dots \quad (3)$$

To look for the right unitary transformation operator  $S$ , we separate the Hamiltonian in Eq. (2) into three parts:  $H_0 = \Omega \sum_i \hat{n}_{i,2}$ ,  $H_1 = H - H_0 - H_2$  and  $H_2 = H'_l$ . To the zeroth order in  $1/\Omega$  the operator  $S^{(1)}$  is given by

$$S^{(1)} = \sum_{i,\alpha>\alpha'} \frac{U^{\alpha,\alpha'}}{4\Omega} \left( b_{i,\alpha}^\dagger b_{i,\alpha'}^\dagger b_{i,\alpha} b_{i,\alpha'} - b_{i,\alpha'}^\dagger b_{i,\alpha}^\dagger b_{i,\alpha} b_{i,\alpha'} \right). \quad (4)$$

One can check that  $S^{(1)}$  satisfies  $[S^{(1)}, H_0] = -H_2$ , so, to the zeroth order in  $1/\Omega$ , the effective Hamiltonian is simply the sum of  $H_0$  and  $H_1$ . The next order operators  $S^{(2)}$  and  $S^{(3)}$  can be found recursively, *e.g.*,

$S^{(2)} = [H_2, H_1]/4\Omega^2$ . Using the canonical transformation defined in Eq. (3) with  $S = S^{(1)} + S^{(2)} + S^{(3)}$ , we decouple  $H$  to the order  $1/\Omega^2$ :  $H_{\text{eff}} = H_0 + H_1 + \frac{1}{2}[S^{(1)}, H_2] + \frac{1}{2}[S^{(2)}, H_2]$ . Then, by projecting  $H_{\text{eff}}$  on the lowest Bloch band, and omitting the band index, we arrive at the following low-energy Hamiltonian to this order:

$$\begin{aligned} \tilde{H}_{\text{eff}} = & \sum_i \left[ \frac{1}{2} \left( \tilde{U} - \frac{pU_{FB}}{2} \hat{n}_i^F \left( \frac{U^{1,2}}{\Omega} \right)^2 \right) \hat{n}_i (\hat{n}_i - 1) - \tilde{\mu} \hat{n}_i \right] + \tilde{H}_t \\ & + \sum_i U_{FB} (\hat{n}_i - \langle \hat{n}_i \rangle) \hat{n}_i^F + H_F. \end{aligned} \quad (5)$$

The tilde indicates the renormalization of the original boson Hubbard parameters  $U$ ,  $t$  and  $\mu$  due to processes involving virtual transitions of the bosons to the higher Bloch band, *e.g.*,  $\tilde{U} = U - (U^{1,2})^2/\Omega + \dots$ . These renormalizations are also present in a pure bosonic system and are independent of  $U_{FB}$ . Most importantly, however, the contact interactions with the fermions provide an additional renormalization to the boson on-site potential  $\tilde{U}$  which is linear in  $U_{FB}$ .

The correction to the boson-boson repulsion due to the fermions corresponds to a virtual process when two bosons are excited from the first to the second Bloch band. The probability for such processes to occur (*i.e.*, the fraction of time the system dwells in such a virtual state) is proportional to  $(U^{1,2}/\Omega)^2 n_i (n_i - 1)$ . While in the virtual state, the interaction energy between the bosons and the fermions (defined by  $H_{BF}$  in Eq. (2)) changes by  $2(U_{BF}^{(2)} - U_{BF}^{(1)}) n_{Fi}$ . Thus, by combining the above two terms and introducing the dimensionless parameter  $p$  (to account for the change in the interaction energy),

$$p = 1 - \langle w_{i,2}; u_i | w_{i,2}; u_i \rangle / \langle w_{i,1}; u_i | w_{i,1}; u_i \rangle, \quad (6)$$

one recovers the correction to the boson-boson repulsion given in Eq. (5). For attractive boson-fermion interactions, the fermionic wavefunction  $u(\mathbf{r})$  is peaked at the center. Thus, the overlap of  $u_i$  with the boson Wannier function in the second Bloch band,  $w_{i,2}$ , is smaller than its overlap with  $w_{i,1}$ . Therefore, for negative  $U_{BF}$ ,  $p$  is positive and  $\mathcal{O}(1)$ . However,  $p$  changes sign for repulsive  $U_{BF}$ , since, in this case, the two species of atoms maximize the distance between them (*i.e.*, the fermion density is suppressed at the center of the unit cell), resulting in the numerator in the second term in Eq. (6) exceeding the denominator. From Eq. (5), notice that the sign of the renormalization to  $\tilde{U}$  is determined by  $\text{sgn}(pU_{FB})$ . Therefore, it remains repulsive and tends to suppress the superfluid phase for either sign of  $U_{BF}$ .

*Shift of the phase diagram:* To the lowest order in  $U_{FB}$ , the on-site interaction energy and the chemical potential of the bosons are modified as  $\tilde{U} \rightarrow U' = \tilde{U} - pU_{FB} (U^{1,2}/\sqrt{2}\Omega)^2 n_{Fi}^0$  and  $\tilde{\mu} \rightarrow \mu' = \tilde{\mu} - U_{FB} n_{Fi}^0$ , with  $n_{Fi}^0$  the average density of the fermions. Since the

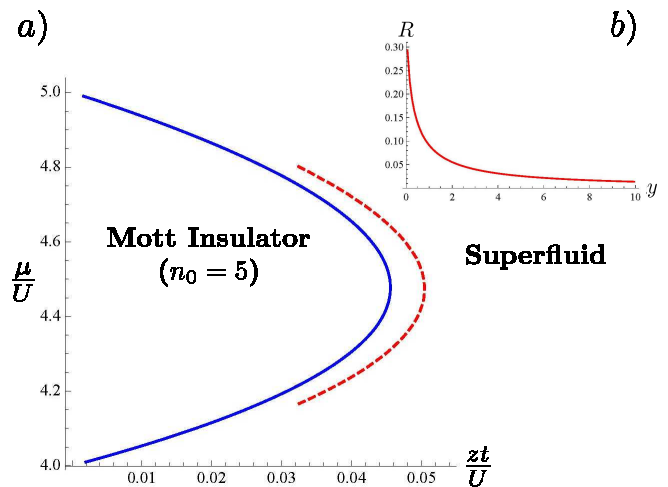


FIG. 1: (Color online) (a) Main panel: Phase Boundary of the boson Hubbard model with and without the fermions for the boson density  $n_0 = 5$ . Solid line describes the insulator-superfluid phase boundary without the fermions. The dashed line corresponds to the phase boundary with the fermions present in the region of the validity of the perturbation series [23]. Here we used  $U_{FB} \approx -U_{BB}$ ,  $U^{1,2}/\Omega \approx 0.3$ ,  $\Delta/U_{BB} = 40$  and  $n_{Fi}^0 = 0.75$ . (b) Inset: The dependence of the function  $R(y)$  on its argument.

fermions appear only at the quadratic order in Eq. (5), integrating them out leads to the effective imaginary-time action [20]

$$\begin{aligned} S_{\text{eff}}(b^*, b) = & \sum_i \int_0^\beta d\tau \left[ b_i^* \partial_\tau b_i + \frac{U'}{2} \hat{n}_i (\hat{n}_i - 1) - \mu' \hat{n}_i \right] \\ & - \int_0^\beta d\tau \tilde{H}_t - \sum_{ij} \int_0^\beta d\tau_1 \int_0^\beta d\tau_2 n_i(\tau_1) M_{ij}(\tau_1 - \tau_2) n_j(\tau_2) \end{aligned} \quad (7)$$

From the last term in Eq. (7), it is clear that the fermions induce a second boson-boson interaction with the spatially and temporally non-local kernel (to the order  $U_{FB}^2/\Delta$ )  $M_{ij}(\tau_1 - \tau_2) = U_{FB}^2 \langle \delta n_{Fi}(\tau_1) \delta n_{Fj}(\tau_2) \rangle / 2$ . Here,  $\delta n_{Fi} = n_{Fi} - n_{Fi}^0$  and the parameter  $\Delta$  is proportional to the inverse of the density of states at the Fermi level  $\nu_F$ ,  $\Delta = 1/\nu_F a^3$ . This contribution describes the screening of the bosonic repulsive interactions by the fermions, which effectively reduces  $U$ , leading to the suppression of the Mott insulating phase [5, 12, 14].

The effect of the above two competing contributions on the phase diagram can be calculated analytically. We first need to calculate the boson on-site Green's function

[21] for the action in Eq. (7) at zero frequency [14],

$$G_i(0) = \quad (8)$$

$$-\frac{n_0+1}{\delta E_p} \left[ 1 + \frac{p U_{FB} n_0 n_{F_i}^0}{2\delta E_p} \left( \frac{U^{1,2}}{\Omega} \right)^2 + \frac{U_{FB}^2 R(\frac{\delta E_p}{4E_F})}{\Delta \delta E_p} \right]$$

$$-\frac{n_0}{\delta E_h} \left[ 1 + \frac{p U_{FB} (1-n_0) n_{F_i}^0}{2\delta E_h} \left( \frac{U^{1,2}}{\Omega} \right)^2 + \frac{U_{FB}^2 R(\frac{\delta E_h}{4E_F})}{\Delta \delta E_h} \right].$$

Here  $\delta E_p$  and  $\delta E_h$  are the particle and the hole excitation energies:  $\delta E_p = U' n_0 - \mu'$  and  $\delta E_h = \mu' - U'(n_0 - 1)$ ,  $n_0$  is the number of bosons per site minimizing the ground state energy. The dimensionless function  $R(y) = -\frac{3}{\pi} \int_0^1 x^2 dx \int_0^\infty d\nu \frac{y}{y^2 + \nu^2} \Pi(x, \nu) / \nu_F$ , where  $\Pi(\mathbf{q}, \Omega_n)$  is the three-dimensional fermion polarization function [22]. The dependence of  $R(y)$  on its argument is plotted in Fig. 1. The mean field SI phase boundary can be obtained by solving the equation [21]

$$\frac{1}{z\tilde{t}} + \int_{-\beta}^{\beta} d\tau G_i(\tau) = 0, \quad (9)$$

where  $z$  is the lattice coordination number.

To the linear order in  $U_{FB}$ , the correction to the phase boundary is influenced only by the enhancement of the on-site repulsion given in Eq. (5):

$$\frac{\delta t^{(1)}}{\tilde{U}} \equiv \frac{t(a_{BF}) - t(a_{BF}=0)}{\tilde{U}} = -\frac{U_{FB} p}{2\tilde{U}} \left( \frac{U^{1,2}}{\Omega} \right)^2 n_F^0 \quad (10)$$

$$\times \left[ \frac{[1 + 2(\tilde{\mu}/\tilde{U})^2 - 2(\tilde{\mu}/\tilde{U})(n_0 - 1) - n_0] n_0}{[1 + (\tilde{\mu}/\tilde{U})^2]} \right]$$

Notice that for either attractive or repulsive  $U_{BF}$ , the product of  $U_{BF}$  and  $p$  remains negative. Therefore, the shift  $\delta t^{(1)}$  is towards shallower lattices, indicating an expansion of the Mott-insulating lobes. The shift of the phase boundary due to the fermion-mediated screening, which manifests itself only in the second order in  $U_{FB}$ , is given by,

$$\frac{\delta t^{(2)}}{\tilde{U}} = -\frac{U_{FB}^2}{\Delta \tilde{U} \left( 1 + \frac{\tilde{\mu}}{\tilde{U}} \right)^2} \quad (11)$$

$$\times \left\{ (n_0+1) \left( \frac{\tilde{\mu}}{\tilde{U}} - (n_0-1) \right)^2 R \left( \frac{\tilde{U}}{4E_F} \left[ n_0 - \frac{\tilde{\mu}}{\tilde{U}} \right] \right) \right.$$

$$\left. + n_0 \left( n_0 - \frac{\tilde{\mu}}{\tilde{U}} \right)^2 R \left( \frac{\tilde{U}}{4E_F} \left[ \frac{\tilde{\mu}}{\tilde{U}} - (n_0-1) \right] \right) \right\}.$$

As expected, the fermion-mediated screening enhances the area occupied by the superfluid phase. Notice that the small perturbation parameters used in the above calculations are  $\frac{U^{12}}{\Omega}$  and  $\frac{U_{FB}}{\Delta}$ , respectively. Therefore, they can be parametrically valid for both  $|U_{BF}|$  smaller as well

as larger than the bare  $U$ . At the tip of the Mott lobes, the ratio of the two contributions for  $n_0 \gg 1$  is given by,

$$\left| \frac{\delta t^{(1)}}{\delta t^{(2)}} \right| \sim \frac{|p| n_F^0 \Delta}{|U_{FB}| n_0 R(\frac{\tilde{U}}{8E_F})} \left( \frac{U^{12}}{\Omega} \right)^2 \quad (12)$$

Since the two competing contributions depend on different *independent* parameters, the sign of the phase boundary shift is a quantitative question. For example, for  $(\frac{U^{12}}{\Omega})^2 \sim \frac{|U_{FB}|}{\Delta}$ , the two effects are comparable. In general, for  $\sqrt{\frac{|U_{FB}|}{\Delta}} < \frac{U^{12}}{\Omega}$ , the superfluid state is suppressed for either sign of the interspecies interaction, as shown in the figure 1.

*Conclusion:* We show that the virtual transitions of bosons to the higher Bloch bands in an optical lattice, coupled with contact interactions with a degenerate gas of fermions, generate a new renormalization of the interactions in the boson Hubbard model. For either sign of the coupling between the fermions and the bosons, this renormalization enhances the boson on-site repulsion, and thus favors the Mott insulating phase. If this effect is dominant over the usual fermion mediated screening, the superfluid coherence of the Bose-Hubbard system will be suppressed by the fermions, as has been observed in recent experiments [2, 3, 4].

We thank L. Cywinski, T. Porto and W. Phillips for stimulating discussions. This work is supported by ARO-DARPA and the Clemson University start-up funds.

- 
- [1] M. P. A. Fisher *et al.*, Phys. Rev. B **40**, 546 (1989).
  - [2] K. Günter *et al.*, Phys. Rev. Lett. **96**, 180402 (2006).
  - [3] S. Ospelkaus *et al.*, Phys. Rev. Lett. **96**, 180403 (2006).
  - [4] Th. Best *et al.*, arXiv:0807.4504 (2008)
  - [5] H. P. Büchler and G. Blatter, Phys. Rev. Lett. **91**, 130404 (2003); Phys. Rev. A **69**, 063603 (2004)
  - [6] M. Lewenstein *et al.*, Phys. Rev. Lett. **92**, 050401 (2004).
  - [7] L. Mathey *et al.*, Phys. Rev. Lett. **93**, 120404 (2004);
  - [8] K. Sengupta, N. Dupuis and P. Majumdar, Phys. Rev. A **75**, 063625 (2007)
  - [9] A. Mering and M. Fleischhauer, Phys. Rev. A **77**, 023601 (2008)
  - [10] C. N. Varney, V. G. Rousseau, R. T. Scalettar, Phys. Rev. A **77**, 041608 (R) (2008).
  - [11] I. Titvinidze, M. Snoek, W. Hofstetter, Phys. Rev. Lett. **100**, 100401 (2008).
  - [12] L. Pollet, C. Kollath, U. Schollwöck, and M. Troyer, Phys. Rev. A **77**, 023608 (2008).
  - [13] G. Refael and E. Demler, Phys. Rev. B **77**, 144511 (2008).
  - [14] R. Lutchyn, S. Tewari and S. Das Sarma, Phys. Rev. B (R), in press (2008); arXiv:0806.2865.
  - [15] D.-S. Luhmann *et al.*, Phys. Rev. Lett. **101**, 050402 (2008)
  - [16] V.W. Scarola, and S. Das Sarma, Phys. Rev. Lett. **95**, 033003 (2005)
  - [17] A. Isacsson and S. M. Girvin, Phys. Rev. A **72**, 053604 (2005)

- [18] W. V. Liu and C. Wu, Phys. Rev. A **74**, 013607 (2006).
- [19] J. R. Schrieffer and P. A. Wolff, Phys. Rev. **149**, 491 (1966).
- [20] When deriving the effective action  $S_{\text{eff}}$  we neglected the term proportional to  $U_{FB}^2/\Omega^4$  since it is much smaller than the last term in Eq. (7).
- [21] S. Sachdev, *Quantum Phase Transitions* (Cambridge University Press, Cambridge, 1999).
- [22] A. L. Fetter and J. D. Walecka, *Quantum Theory of Many-Particle Systems* (McGraw-Hill, New York, 1971).
- [23] Near the degeneracy points [21] where  $\delta E_{p/h}$  is of the order of  $U_{FB}^2/\Delta$  the perturbation theory breaks down.